CXCR4 Inhibition with AMD3100 Sensitizes Prostate Cancer to Docetaxel Chemotherapy[1]

Urszula M. Domanska*, Hetty Timmer-Bosscha*, Wouter B. Nagengast*, Thijs H. Oude Munnink*, Roeliene C. Kruizinga*, Hildo J.K. Ananias[†], Nathalie M. Kliphuis*, Gerwin Huls[‡], Elisabeth G.E. De Vries*, Igle J. de Jong[†] and Annemiek M.E. Walenkamp*

*Department of Medical Oncology, University Medical Center Groningen, Groningen, The Netherlands; [†]Department of Urology, University Medical Center Groningen, Groningen, The Netherlands; [‡]Department of Haematology, University Medical Center Groningen, Groningen, The Netherlands

Abstract

Several *in vitro* and *in vivo* models have revealed the key role of CXCR4/CXCL12 axis in tumor-stroma interactions. Stromal cells present in the tumor microenvironment express high levels of CXCL12 protein, directly stimulating proliferation and migration of CXCR4-expressing cancer cells. This specific prosurvival influence of stromal cells on tumor cells is thought to protect them from cytotoxic chemotherapy and is postulated as a possible explanation for the minimal residual disease in hematological and solid cancers. Therefore, CXCR4/CXCL12 signaling is an attractive therapeutic target in cancer, as proven in preclinical leukemia mouse models, where CXCR4 inhibition sensitized cancer cells to conventional chemotherapy. This study investigates whether inhibition of CXCR4 with the specific inhibitor AMD3100 sensitizes human prostate cancer cells to docetaxel. We showed that both mouse and human stromal cell lines have a protective effect on PC3-luc cells by promoting their survival after chemotherapy. Furthermore, we demonstrated that AMD3100 sensitizes PC3-luc cells to docetaxel. In a subcutaneous xenograft mouse model of human prostate carcinoma, we showed that a combination of docetaxel and AMD3100 exerts increased antitumor effect compared with docetaxel alone. We concluded that CXCR4 inhibition chemosensitizes prostate cancer cells, both *in vitro* and *in vivo*. To explore the relevance of these findings, we analyzed CXCR4 expression levels in human prostate cancer samples. We found that cancer cells present in bone metastatic lesions express higher CXCR4 levels relative to the cells present in primary tumors and lymph node metastatic lesions. These findings underscore the potential of CXCR4 inhibitors as chemosensitizing agents.

Neoplasia (2012) 14, 709–718

Introduction

The pivotal role of the chemokine receptor 4 (CXCR4) and its ligand (CXCL12) in the proliferation and metastasis of tumor cells, induction of angiogenesis, and invasive tumor growth has been recognized for over a decade [1]. CXCR4 expression is an independent prognostic factor for poor overall survival not only in prostate cancer [2] but also in melanoma [3] and metastatic colorectal cancer [4]. In patients with breast cancer, a high expression of CXCR4 is associated with poor survival [5].

Stromal cells are thought to be a major source of CXCL12. In the bone marrow, constitutive CXCL12 secretion by stromal cells is crucial for homing and sustaining CXCR4-expressing hematopoietic stem and progenitor cells (HSCs and HPCs) in their niches [6,7]. As shown in acute myeloid leukemia (AML) human xenotransplant mouse models, leukemic cells also localize in CXCL12-rich niches of bone marrow, where the protective microenvironment favors their growth and survival during cytotoxic treatment [8]. In murine models of chronic myelogenous leukemia [9], acute myeloid leukemia [10], and chronic lymphocytic leukemia [11], it has been shown that CXCR4 antagonists—such as the small-molecule AMD3100 (plerixafor—a drug that blocks the binding pocket of CXCR4), CXCL12 analogs (CTCE-9908), and T140 analogs (peptidic CXCR4 antagonists)—can disrupt tumor-stroma interactions and mobilize leukemic cells to the peripheral blood, making them more sensitive to conventional anticancer drugs.

Interestingly, solid tumors also interact with the stromal microenvironment. In metastatic mouse models of osteosarcoma and melanoma [12] and in a transgenic breast cancer mouse model [13], it is shown that cancer cells metastasize preferentially to CXCL12-rich niches. A study in a prostate cancer mouse model revealed that prostate cancer homes to the bone marrow through CXCR4/CXCL12 axis by competing with hematopoietic stem cells for the endosteal niches, from where both cell types can be mobilized by CXCR4 inhibition [14]. Also, in a human breast cancer xenograft mouse model, in which cancer-associated fibroblasts were coimplanted, it was shown that breast cancer cells actively recruit stromal cells to the tumor, which, in turn, recruit CXCR4-positive bone marrow–derived progenitor cells. This stimulates angiogenesis and vasculogenesis and supports tumor growth [15]. Strikingly, cancer-associated fibroblasts, but not normal fibroblasts, were shown to have the ability to promote progression of tumorigenesis of prostate epithelium *in vivo* and in an *in vitro* coculture system [16].

The cancer cell microenvironment has recently become a topic of interest in prostate cancer research as well. Prostate cancer is the most common cancer in men and the second leading cause of cancer-related death in Western countries [17]. The treatment of localized prostate cancer consists of surgery or radiotherapy with or without hormonal therapy, whereas in advanced disease, hormonal therapy based on androgen depletion is indicated [18,19]. For castrate-refractory prostate cancer patients with advanced disease, standard chemotherapy regimens with docetaxel [20] and cabazitaxel are available [21]. However, the castrate-refractory prostate cancer has a striking preference for skeletal localization of distant metastasis [22]. It has been postulated that the bone marrow stromal microenvironment provides a protective niche for cancer cells, leading to therapy resistance and possibly relapse of disease [23]. Therefore, novel treatment options in prostate cancer, which target the cancer cell–microenvironment interaction, are of interest.

In this study, we questioned whether targeting the CXCR4/CXCL12 axis in prostate cancer interferes with the protective tumor-stromal microenvironment interactions and sensitizes cancer cells to docetaxel chemotherapy. Moreover, we aimed to explore the potential relevance of our findings by analyzing CXCR4 expression levels in patient samples of primary and metastatic prostate cancer.

Materials and Methods

Cell Lines
Luciferase-transfected human metastatic prostate cancer cell line (PC3-luc; Caliper Life Sciences, 'S-Hertogenbosch, the Netherlands) was cultured in Roswell Park Memorial Institute (RPMI) 1640 medium with 10% fetal bovine serum (FBS; Perbio Sciences, Breda, the Netherlands) and the breast cancer cell line (MDA-MB-231; ATCC, Wesel, Germany), included as a positive control, was cultured in Dulbecco modified Eagle medium with 10% FBS and 1% L-glutamine. Human bone marrow–derived stromal cell line (HS27a; ATCC) was maintained in RPMI 1640 with 10% FBS and the mouse bone marrow–derived stromal fibroblasts cell line (MS5; ATCC) in α-minimum essential medium with 10% FBS. All cell lines were maintained at 37°C with 5% CO_2 in a humidified atmosphere. All media and supplements were obtained from Invitrogen (Bleiswijk, the Netherlands).

Drug Sensitivity in the In Vitro Coculture Model
PC3-luc cells (or control cells MDA-MB-231) cells prelabeled with red fluorescent dye (DiI; Invitrogen) were plated in 24-well plates on glass slides with or without precultured stromal monolayer (MS5 or HS27a). Cells were treated with docetaxel (LC Laboratories, Woburn, MA) in concentrations ranging from 0.1 to 1 μM for 40 hours with or without 25 μg/ml AMD3100 (Sigma, Zwijndrecht, the Netherlands) or with docetaxel with or without a 1:100 anti-hCXCL12 antibody (cross-reactive with mouse CXCL12 according to datasheet specifications; Abcam, Cambridge, United Kingdom). Glass slides were collected after treatment, fixed, and stained with 4′,6-diamidino-2-phenylindole (DAPI; Sigma). Tumor cell viability was assessed with nuclear DAPI staining based on the observation of the nuclear structure (intact *vs* fragmented nuclei). DiI staining was used to identify tumor cells in coculture.

Cell Adhesion in the In Vitro Coculture Model
PC3-luc cells prelabeled with DiI were plated in 24-well plates on glass slides with MS5 monolayer in the presence or absence of 25 μg/ml AMD3100. The glass slides were collected and fixed at 0 to 24 hours. The total number of adherent tumor cells was counted by fluorescent microscopy.

Cell Migration Assay
Transwell inserts (pore size, 8 μm) and lower wells were coated with 15 μg/ml collagen type I, incubated for 1 hour at 37°C and blocked overnight with phosphate-buffered saline (PBS) containing 1% bovine serum albumin at 4°C. Subsequently, the blocking buffer was removed, and the lower wells were loaded with 300 μl of 10^{-7} M CXCL12 in serum-free RPMI or serum-free RPMI only (negative control).

PC3-luc cells were serum-starved overnight and harvested with enzyme-free cell detaching buffer. The cells were incubated with 25 μg/ml AMD3100 in serum-free RPMI or serum-free RPMI only for 30 minutes at 37°C. Inserts were loaded with 12×10^4 cells in 150 μl per condition and were allowed to migrate for 4.5 hours at 37°C. After migration, nonmigrated cells were removed with a cotton swab wetted in PBS. Cells at the bottom surface were fixed in 75% methanol/25% acidic acid for 20 minutes at room temperature, stained with 0.25% Coomassie blue in 45% methanol/10% acidic acid for 20 minutes at room temperature, washed, air-dried, and mounted on a microscope slide. The number of migrated cells was calculated by counting cells from five fields of view per slide, with 40× magnification with a counting grid.

CXCR4 Membrane Expression
PC3-luc or MDA-MB-231 cells were incubated with 1:100 polyclonal rabbit anti-hCXCR4 antibody (Abcam) or with PBS (2.7 mM KCl, potassium 1.8 mM KH_2PO_4, 137 mM NaCl, 10.1 mM Na_2HPO_4,

pH 7.4) for 45 minutes on ice, followed by 30 minutes of incubation with mouse–anti rabbit antibody phycoerythrin-labeled (Southern Biotech, Uithoorn, the Netherlands) and measured by FACSCalibur (Epics Elite; Coulter Electronics, Mijdrecht, the Netherlands). Data analysis was performed using Kaluza software (Beckman Coulter Nederland BV, Woerden, the Netherlands).

CXCL12 Enzyme-Linked Immunosorbent Assay

Medium from confluent MS5, HS27a, PC3-luc, and MDA-MB-231 cell lines were sampled at 48 hours after plating in 24-well plates and centrifuged to remove cell debris. CXCL12 levels in medium were assayed with the Quantikine Human CXCL12/SDF1α Immunoassay

kit (R&D Systems, Abingdon, United Kingdom) according to the manufacturer's instructions. Measured levels were expressed as picograms CXCL12 per 1 mg of protein in cell lysate.

Cell Viability Assay

PC3-luc cells were plated in 96-well plates and allowed to attach for 3 to 5 hours and then the medium was exchanged for MS5-derived culture supernatant and cells were treated with increasing docetaxel concentrations (0.1-1 µM) alone or combined with 25 µg/ml AMD3100 or 1:100 anti-hCXCL12 antibody. Survival of cells at day 3 was assessed by 1-(4,5-dimethylthiazol-2-yl)-3,5-diphenylformazan (MTT; Sigma) as described previously [24].
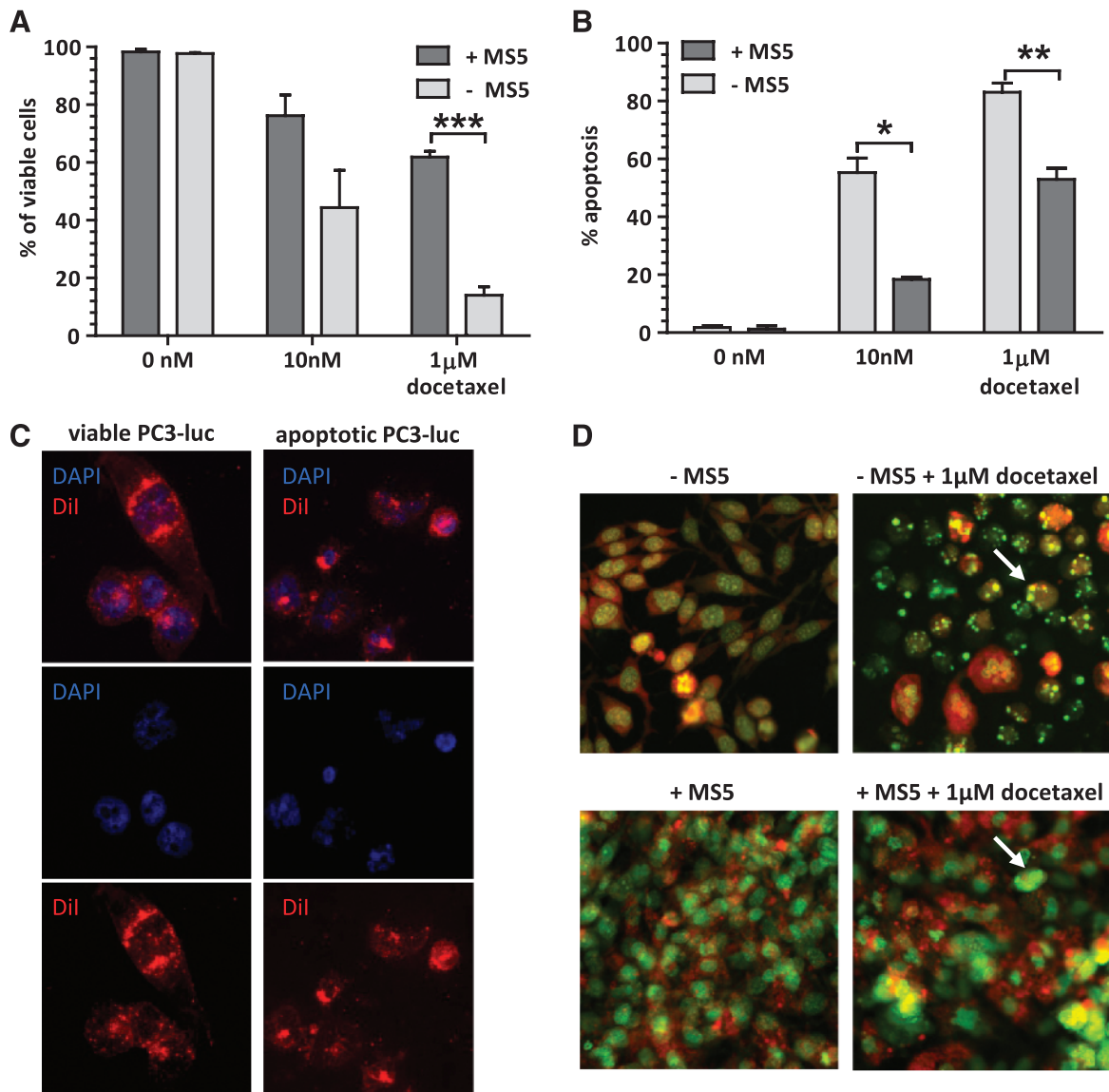

Figure 1. (A) Viability of PC3-luc cells after docetaxel treatment with or without the presence of MS5 stromal cell line. (B) Apoptosis of PC3-luc cells after docetaxel treatment with or without MS5 stromal cell line. (C) Exemplary figures presenting the assessment of PC3-luc cell viability by fluorescence microscopy (40×). The nuclei (blue, DAPI) are round and intact with visible nucleoli in viable cells, whereas nuclei of apoptotic PC3-luc cells are condensed and fragmented. Cytoplasm visualized in red (DiI) shows regular structure in viable cells, whereas it is condensed in apoptotic cells. (D) Exemplary pictures representing the assessment of apoptosis of PC3-luc cell line obtained by fluorescence microscopy (40× magnification). Apoptotic cells, defined by chromatin condensation and presence of apoptotic bodies, are indicated by arrows. *P < .05, **P < .005, ***P < .0005.
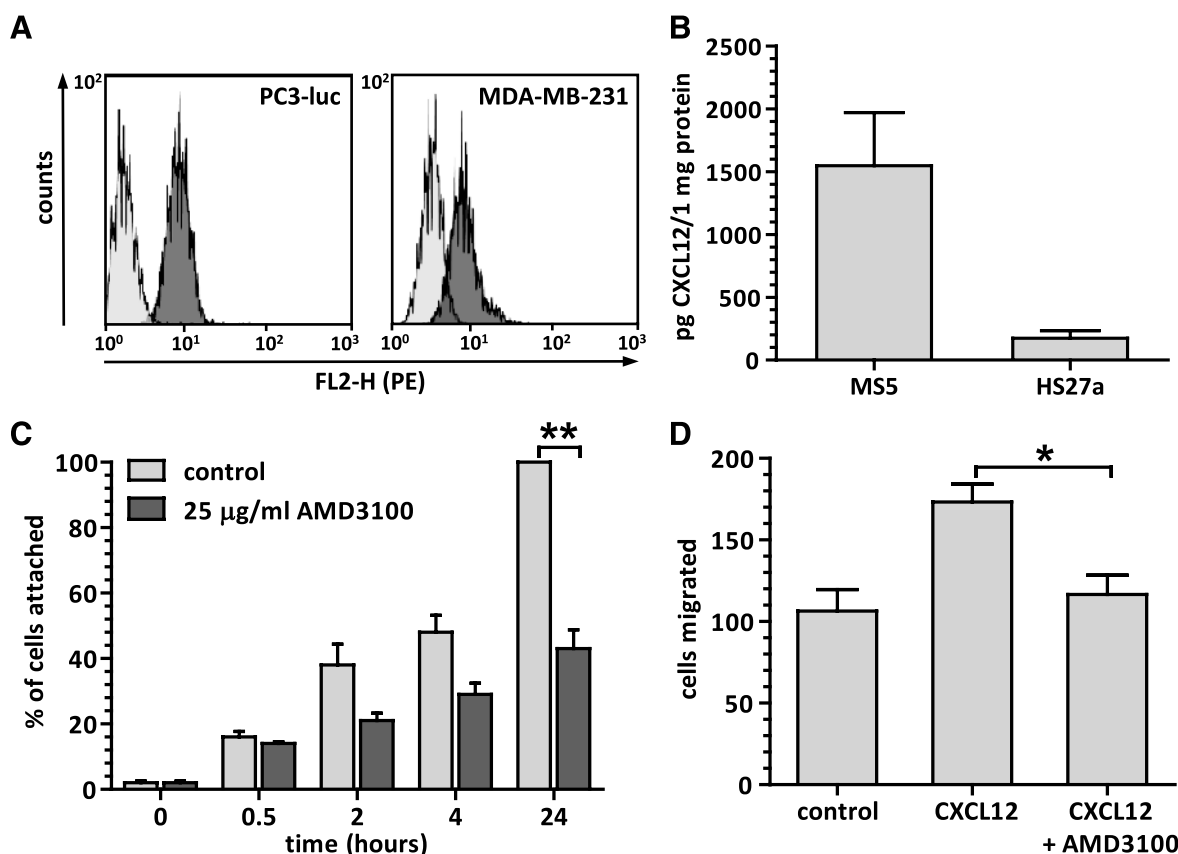
Figure 2. (A) Membrane expression of CXCR4 on PC3-luc (left panel) and MDA-MB-231 (right panel) cancer cell lines presented as mean fluorescence intensity (FL2-H/PE) of cells stained with (dark-gray histogram) or without (light-gray histogram) CXCR4 antibody. (B) Constitutive levels of CXCL12 produced by mouse (MS5) and human (HS27a) stromal cell lines. (C) Adhesion of PC3-luc cells to the layer of murine stromal cells (MS5) in time, in the presence or absence of 25 μg/ml AMD3100. (D) Quantification of PC3-luc cell migration toward 10^{-7} M CXCL12 with or without 25 μg/ml AMD3100. *P = .005, **P = .0001.

Apoptosis Assay

PC3-luc cells were plated in 96-well plate with or without precultured MS5 stromal monolayer. Once attached, cells were treated with increasing docetaxel concentrations (0.1-1 μM) alone or combined with 25 μg/ml AMD3100 or 1:100 anti-hCXCL12 antibody. MS5 cells alone were treated with all conditions as well to assess the background level of apoptosis of stromal cells. After 40 hours, acridine orange was added to each well to distinguish apoptotic from viable cells. The intensity of apoptotic staining was assessed by fluorescence microscopy, and apoptosis was defined based on the chromatin condensation and presence of apoptotic bodies. For every condition in coculture, the background level of stromal cells apoptosis was extracted to assess the apoptosis of PC3-luc cells only. At least 300 PC3-luc cells per condition were scored. Results are expressed as a percentage of apoptotic cells.

Tumor Xenografts and In Vivo Treatment

Male Hsd:Athymic Nude-*Foxn1*[nu] 6 to 8 weeks old were injected subcutaneously with 3 × 10^6 PC3-luc cells in 100 μl of PBS into the dorsal region. Tumor size was measured three times per week with a caliper. All experiments were performed under anesthesia by isoflurane inhalation (3% for induction, 1.5% for maintenance) and approved by the ethical committee of the University of Groningen, the Netherlands. At day 14 after inoculation, tumors were established (ranging from 100 to 200 mm^3, calculated as 100% of tumor size), and mice were randomized into four treatment groups: 1) sterile water intraperitoneally (ip)

daily five times per week (control group, n = 9), 2) docetaxel 10 mg/kg ip once weekly and sterile water ip on the remaining 4 days (n = 5), 3) AMD3100 3.5 mg/kg ip daily five times per week (n = 9), and 4) combination treatment of docetaxel and AMD3100 (n = 6). After 5 weeks of treatment, or when humane end points (ulceration or tumor size >2 cm^3) were reached, animals were killed and tumors were excised, weighed, formalin-fixed and paraffin-embedded (FFPE), and subjected to immunohistochemical staining with rabbit anti–human CXCR4 and mouse anti–human CXCL12 antibodies (Abcam).

Bioluminescent Imaging of Tumor Growth

Tumors were imaged twice weekly with an IVIS bioluminescent camera (Caliper Life Sciences) 10 minutes after injection with 150 mg/kg D-luciferin (Caliper Life Sciences) with the following camera settings: f/stop1, small binning, and 10 seconds of exposure time. Data were analyzed with LivingImage 3.0 (Caliper Life Sciences).

Human Tumor Tissue Collection and Immunohistochemical Staining

Archival tissue specimens from primary prostate tumors, lymph node, and bone metastases were obtained from the University Medical Center Groningen in the Netherlands. Primary prostate cancer tissues (Gleason stage 6-9) were randomly selected from 15 radical prostatectomies between 2009 and 2010. Bone metastasis specimens (Gleason stage 8-10) of 15 patients were randomly obtained as biopsies for a

single metastatic lesion or from tumor tissue obtained after neurosurgery or orthopedic surgery in symptomatic bone metastases. Lymph node metastatic tissue (Gleason score 6-10) was randomly obtained from nodal staging in 15 patients between 2005 and 2007. Only clinical cases without neoadjuvant androgen deprivation were selected. All tissue specimens were encoded with unique numbers. According to Dutch law, no further institutional review board approval was required (www.federa.org).

FFPE tissue specimens were mounted on slides as a whole tissue sections and stained with hematoxylin and eosin. CXCR4 expression was assessed by staining with rabbit anti-human CXCR4 antibody (Abcam), secondary goat anti-rabbit antibody conjugated to peroxidase (DAKO, Heverlee, Belgium), and subsequent tertiary rabbit anti-goat conjugated to peroxidase (DAKO). Staining was visualized by 3,3′-diaminobenzidine. FFPE cervical cancer cells (HeLa) overexpressing CXCR4 served as a positive control.

Quantification of Immunohistochemical Staining

The intensity of CXCR4 and CXCL12 staining was semiquantitatively scored in scale ranging from 0 (no staining), 1 (weak intensity), 2 (moderate intensity), to 3 (strong intensity) in five randomly dis-

tributed fields of view (40×) per sample. Subsequently, whole samples were classified as positive or negative, based on the sum of all intensity scores per specimen. When the sum of all scores per sample was higher than 5, the sample was defined as CXCR4- or CXCL12-positive.

Statistical Analysis

All *in vitro* experiments were repeated three times. Results were expressed as mean ± SD. Statistical analysis was performed using the 2-tailed t test for parametric data or with χ^2 test for categorical values. $P < .05$ was considered statistically significant. Statistical analysis was performed with GraphPad Prism 5 software.

Results

Stromal Cells Protect Prostate Cancer Cells from Docetaxel-Induced Cytotoxicity

The influence of stromal cells on viability of PC3-luc on docetaxel (Figure 1, *A* and *C*) was evaluated with a fluorescence-based cell viability assay. PC3-luc cells cultured alone were sensitive to docetaxel in
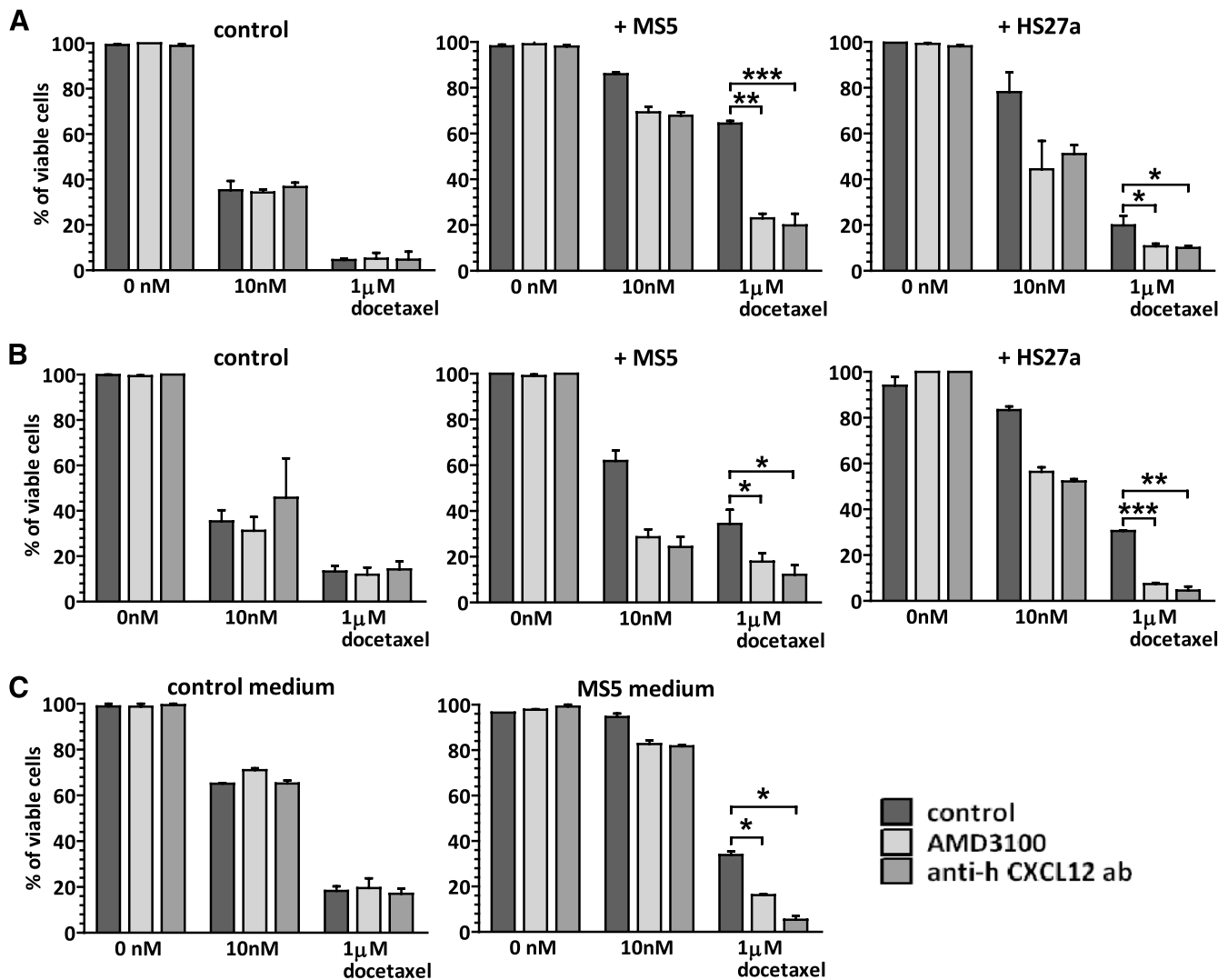

Figure 3. (A, B) Viability of PC3-luc (A) or MDA-MB-231 (B) cells, cultured alone (left panels), with MS5 stromal cell lines (middle panels) or with HS27a stromal cell line (right panels) and treated for 40 hours with docetaxel alone or in combination either with AMD3100 or with anti-CXCL12 antibody. (C) Viability of PC3-luc cells cultured with MS5-derived medium after treatment with docetaxel alone or in combination with AMD3100 or CXCL12 antibody assessed by MTT assay. *P < .5, **P = .005, ***P < .0005.
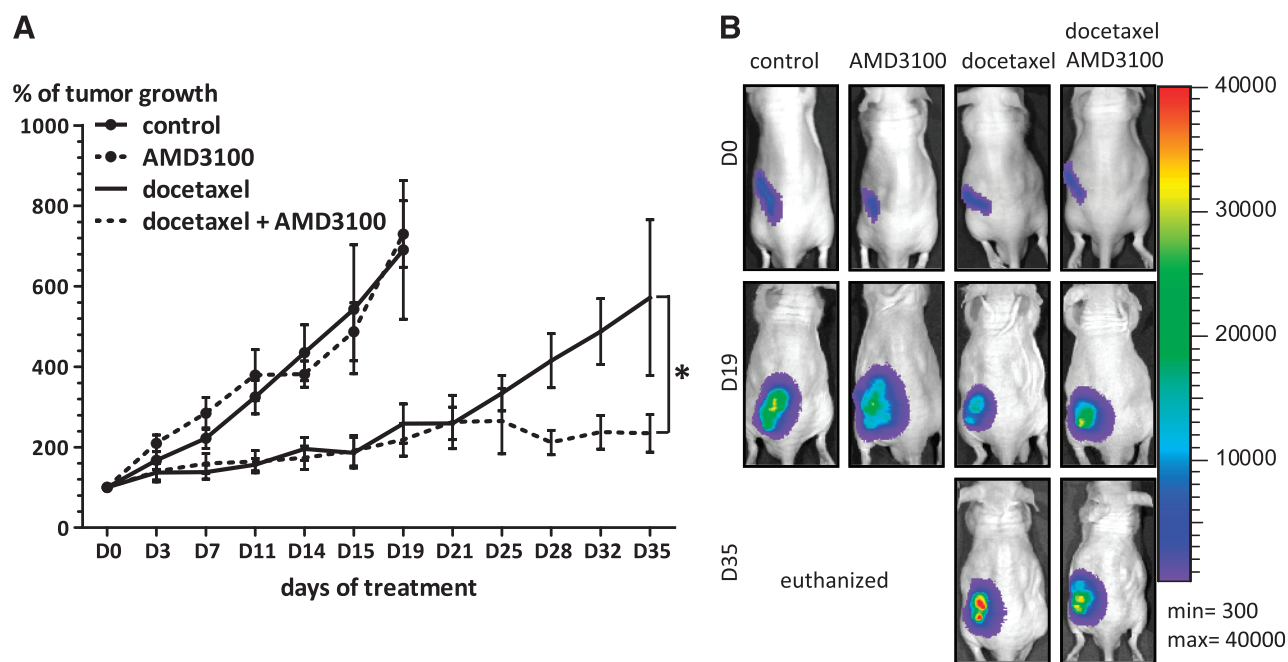
A

B

Figure 4. (A) Tumor volumes expressed as a percentage of tumor growth related to volume at the start of treatment. *P = .01. (B) Representative BLI images of mice from respective treatment groups at days 0, 19, and 35 after the start of treatment.

a dose-dependent manner with a survival of 14% ± 5.1% at 1 µM docetaxel. In contrast, prostate cancer cells showed much higher levels of viability in the presence of stroma (P < .0001). After incubation with 1 µM docetaxel, 61.8% ± 3.4% viable cells remained.

The stromal layer seemed to protect PC3-luc cells by preventing induction of their apoptosis on chemotherapy (Figure 1, *B* and *D*). At 1 µM docetaxel, 83% ± 5.5% apoptosis in PC3-luc cultured alone compared with 53% ± 6.5% apoptosis in PC3-luc in the presence of mouse stromal monolayer (P < .005) was found.

Tumor-Stroma Interactions in Coculture Are CXCR4/ CXCL12 Dependent

The expression of CXCR4 on PC3-luc was shown by FACS analysis (Figure 2*A*), where the mean fluorescence intensity (MFI) reached 9.83 ± 2.5, whereas the MFI of the control sample was 2.31 ± 0.7 (P = .0001). The CXCR4-expressing breast cancer cell line MDA-MB-231 served as control (MFI 15.20 ± 1.34 *vs* MFI of negative control 3.96 ± 0.93, P = .0005). Moreover, as shown by ELISA assay, CXCL12 was constitutively expressed in culture medium derived from both MS5 (1547.42 ± 731.89 pg/1 mg protein) and HS27a (173.74 ± 106.18 pg/1 mg protein) cell lines (Figure 2*B*). Both in the PC3-luc and MDA-MB-231 cell culture media, CXCL12 levels were below the mean minimum detectable dose of the ELISA kit, given as 18 pg/ml (data not shown).

Next, the interaction between stromal cells and PC3-luc in a co-culture model was shown to be CXCR4 dependent in a cell adhesion assay. About 100% of PC3-luc cells were attached to the stroma layer 24 hours after plating, Treatment with 25 µg/ml AMD3100 reduced the percentage of PC3-luc cells attached to the stroma layer to 43.0% ± 9.7% (P < .0001) at 24 hours (Figure 2*C*). As the primary function of the CXCR4 receptor expressed on prostate cancer cells is induction of cell migration, the Transwell migration assay was performed to test the receptor functionality (Figure 2*D*). PC3-luc cells migrated toward the gradient of CXCL12 (173 ± 19 cells migrated), and this process

could be inhibited (P = .02) by preincubating the cells with 25 µg/ml AMD3100 (116 ± 20 cells migrated).

CXCR4/CXCL12 Inhibition Sensitizes Prostate Cancer Cells to Docetaxel Treatment *In Vitro*

To show that the reduced docetaxel cytotoxicity in the presence of stroma was related to the CXCR4/CXCL12 axis, the docetaxel treatment was combined with 25 µg/ml AMD3100 (Figure 3*A*, *left and middle panels*). The addition of AMD3100 abolished the protective stroma effect and decreased PC3-luc cell viability levels again to 19.9% ± 8.7% (P = .001). Similarly, the inhibition of CXCL12 with anti-CXCL12 antibody resulted in sensitization of prostate cancer cells to docetaxel in the presence of stromal cells (P < .0001). In PC3-luc cells cultured alone, no differences in cell viability were found between treatments with docetaxel alone and combined with AMD3100 or anti-CXCL12 antibody. These results were confirmed by the apoptosis assay, where CXCR4/CXCL12 inhibition sensitized PC3-luc cocultured with mouse stromal cell line to docetaxel (data not shown).

Human bone marrow–derived stromal fibroblasts HS27a cell line (Figure 3*A*, *right panel*) was also shown to protect PC3-luc for docetaxel-induced cytotoxicity (19% ± 6% of viable cells in the presence of HS27a *vs* 4% ± 1% of viable tumor cells in the absence of HS27a) after 1 µM docetaxel treatment (P = .02). The stromal protection from docetaxel was neutralized both by treatment with AMD3100, lowering PC3-luc cell viability to 10% ± 2% (P = .04), and by anti-CXCL12 antibody, resulting in 10% ± 1.7% of viable cells (P = .049).

The same role of CXCR4/CXCL12 signaling in the stromal cell–mediated effect was shown for the MDA-MB-231 breast cancer cell line (Figure 3*B*). MDA-MB-231 cells treated with docetaxel showed 12% ± 4% viable cells after 1 µM docetaxel (*left panel*). However, in the presence of MS5 stroma cells, 39% ± 8% of MDA-MB-231 cells remained viable cells after 1 µM docetaxel (P = .01). Both AMD3100 and anti-CXCL12 antibody treatment in the presence of mouse stroma seemed to sensitize breast cancer cells (*middle panel*); tumor cell viability fell to

21% ± 7% (P = .04) and 12% ± 6% (P = .02). This sensitizing effect was absent when MDA-MB-231 cells were cultured alone. Similar results were observed when MDA-MB-231 cells were cocultured with human stromal cells (*right panel*). Both AMD3100 (P = .0005) and anti-CXCL12 (P = .004) antibody sensitized breast cancer cells to docetaxel.

Finally, the conditioned medium of mouse stroma cells harvested after 48 hours of culture seemed to protect PC3-luc cells from docetaxel (Figure 3*D*), and this effect could be reversed by treatment with both CXCR4 inhibitor (P = .006) and with CXCL12-blocking antibody (P = .008), as shown by MTT assay.

AMD3100 Sensitizes Prostate Cancer to Docetaxel In Vivo

Finally, to prove a role of CXCR4/CXCL12 signaling in chemo-sensitivity of prostate cancer cells in the *in vivo* setting, treatment of docetaxel was combined with AMD3100 in a subcutaneous xenograft model of prostate cancer (Figure 4). After 19 days, mice treated with placebo or AMD3100 had reached the defined humane end point because of tumor size (>2 cm^3) and/or tumor ulceration. Mice treated with docetaxel and the combination of docetaxel and AMD3100 showed delayed tumor growth compared with that of the control group (P < .04 and P < .03, respectively). Tumors in mice treated with docetaxel or the combination of docetaxel and AMD3100 were initially, until 21 days, growing at comparable rates. Thereafter, tumors in mice treated with docetaxel continued growing, reaching 572% ± 193% of the initial tumor size at the end of experiment (day 35), whereas tumors treated with the combination of docetaxel and AMD3100 grew slower, reaching 235% ± 47% of the initial tumor size (P = .01).
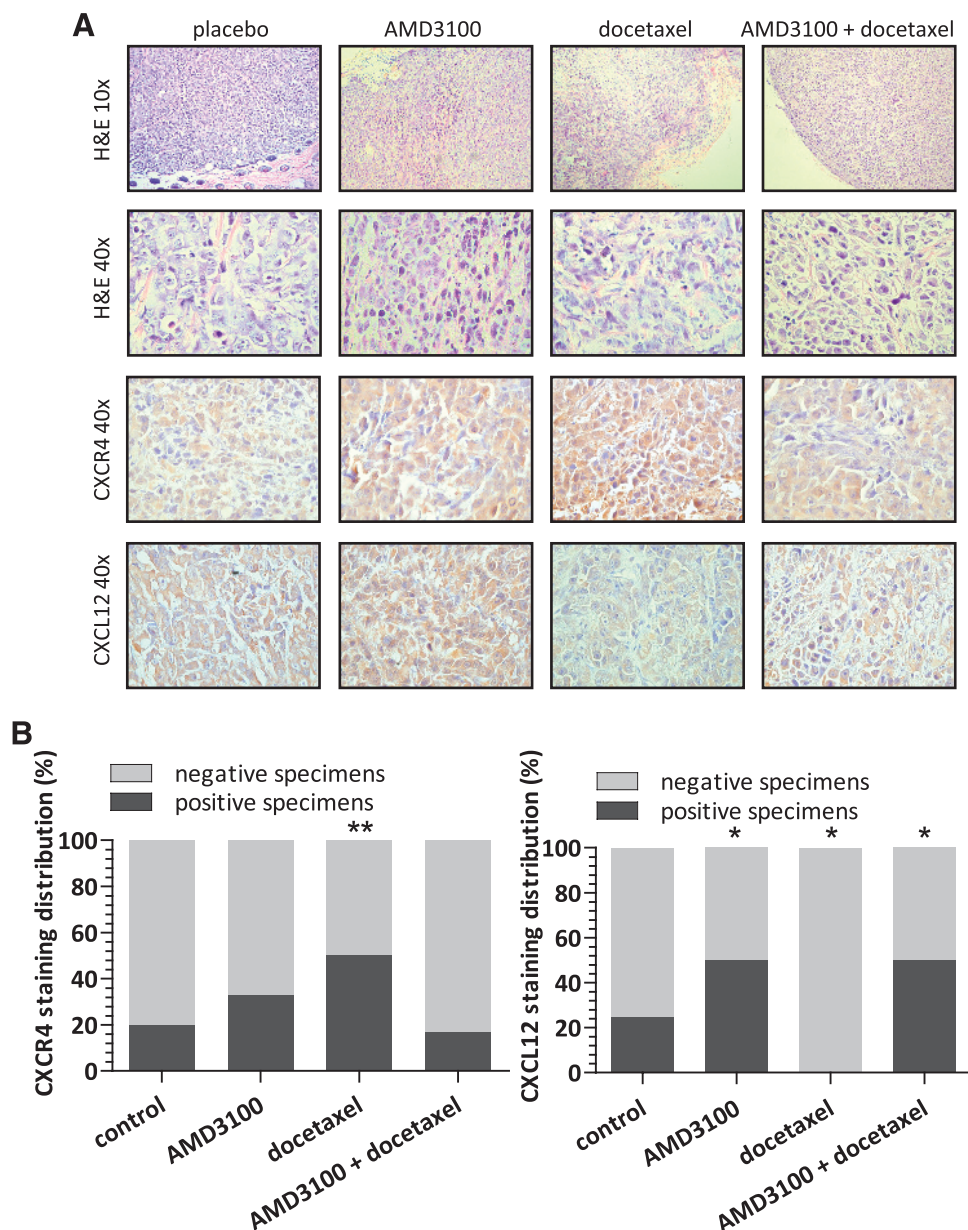

Figure 5. (A) Representative images of immunohistochemical staining of PC3-luc xenografts with hematoxylin and eosin, CXCR4 and CXCL12 (as indicated in rows) from respective treatment groups (as indicated in columns). (B) Quantification of CXCR4 (left panel) and CXCL12 (right panel) staining. *P ≤ .0004, **P < .0001 compared with control.
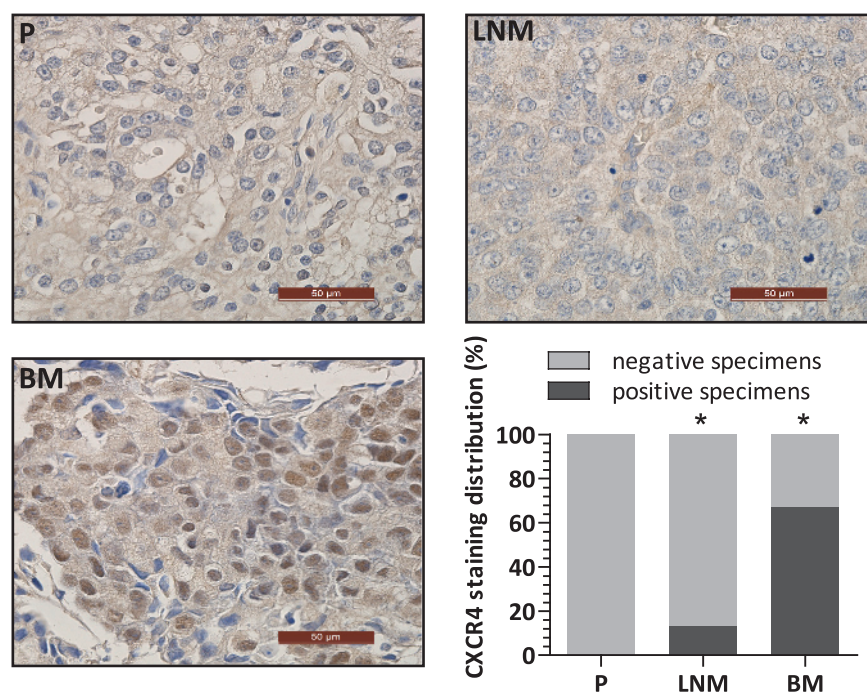
Figure 6. Representative images of CXCR4 immunohistochemical staining on human prostate cancer specimens from primary tumors (P), lymph node metastasis (LNM), and bone metastasis (BM) and quantification of CXCR4 staining in respective lesions (lower right panel). *$P \leq .0002$ compared with primary tumor.

Docetaxel Therapy Causes Increased CXCR4 Expression in Prostate Cancer Cells In Vivo

Although mice were only engrafted with solid tumors, histology of the excised tumors revealed that the tumors were extensively invaded by spindle-shaped stromal cells with small nuclei (Figure 5). CXCR4 staining revealed that only 20% of specimens from the control group showed CXCR4 expression, whereas in docetaxel-treated group 50% of samples were CXCR4-positive ($P < .0001$). CXCL12 staining showed that, in 25% of control tumor specimens, CXCL12 was expressed, whereas after treatment with AMD3100 alone or in combination with docetaxel, CXCL12 expression was present in 50% of specimens ($P = .0004$). In the docetaxel-treated group, all the tumor specimens were CXCL12-negative ($P < .0001$ vs control).

Bone Metastatic Lesions from Prostate Cancer Patients Show Increased Expression of CXCR4

Finally, the expression of CXCR4 in unpaired human prostate cancer specimens obtained from primary tumors, lymph node, and bone metastases was analyzed. Immunohistochemical staining showed that all the specimens from primary prostate cancer lesions were CXCR4-negative, whereas 13% of the samples derived from lymph node metastatic lesions showed cytoplasmic CXCR4 staining ($P = .0002$ vs primary tumor samples). Strikingly, 67% of the bone marrow specimens with tumor involvement showed CXCR4 expression ($P < .0001$ vs primary tumors). Notably, as shown in Figure 6, nuclear localization of CXCR4 was observed in tumor cells present in the bone lesions, as opposed to primary and lymph node–localized tumor cells, which showed mainly cytoplasmic staining.

Discussion

In this study, we demonstrated that the stromal microenvironment protects PC3-luc prostate cancer cells from docetaxel chemotherapy.

Inhibition of CXCR4 with AMD3100 sensitized prostate cancer cells for docetaxel in the presence of stromal cells in in vitro and in vivo models. Moreover, our exploratory study in prostate cancer patient specimens showed that CXCR4 is upregulated in bone marrow metastatic lesions compared with primary lesions and lymph node metastases.

The chemoprotective role of stromal cells has been widely acknowledged as one of the crucial factors directing the response of various types of cancer cells to conventional treatment [23]. Soluble factors released by stromal cells, such as CXCL12, attract CXCR4-expressing cancer cells to the stromal microenvironment. Here, they are exposed to multiple stroma-derived factors, including interleukin 6 and transforming growth factor β, which have been shown to exert a prosurvival effect on breast, pancreatic, and melanoma tumor cells [25–27]. In this way, the specific microenvironmental niche protects CXCR4-expressing cancer cells from genotoxic stress, such as chemotherapy [23,28]. Indeed, several preclinical in vivo studies with leukemic mouse models have demonstrated that interaction of CXCR4-positive leukemic cells with the CXCL12-rich bone marrow microenvironment protects leukemic cells from chemotherapy [6,10]. Interestingly, prostate cancer cells, like CXCR4-expressing leukemic cells, are also home to the CXCL12-expressing niches [14,28,29]. On the basis of this, we postulated that stromal microenvironment protects prostate cancer cells from chemotherapy through CXCR4/CXCL12 interaction.

Our study has shown that both mouse and human bone marrow–derived stromal cells protect prostate cancer cells from docetaxel-induced toxicity in vitro. Moreover, we have demonstrated that the interaction between prostate cancer cells and stroma is CXCR4/CXCL12 dependent and that it is directly conferred by soluble CXCL12 released by stromal cells. Our results are supported by a recently published study, in which in a prostate cancer mouse model CXCR4-positive tumor cells were shown to home in to the CXCL12-rich bone marrow niche [14].

To test whether targeting CXCR4 sensitizes prostate cancer cells to chemotherapy by disrupting their CXCR4/CXCL12–dependent interaction with stroma, we used AMD3100, a CXCR4 inhibitor approved by the Food and Drug Administration. AMD3100 is used for mobilization of HSCs from the bone marrow to peripheral blood in non–Hodgkin lymphoma and multiple myeloma [30]. It exerts the mobilization effect by blocking the CXCR4-dependent interaction between HSCs and bone marrow stroma. In our *in vitro* model, indeed, AMD3100 disrupted the interaction between prostate cancer cells and bone marrow stroma, sensitizing the former to docetaxel. Our xenograft models showed that this finding persisted in the *in vivo* setting by showing a clear chemosensitizing effect of CXCR4 inhibition in mice treated with a combination of AMD3100 and docetaxel. Treatment with AMD3100 alone did not affect the tumor growth. Studies investigating the direct effect of drugs interfering with the CXCL12/CXCR4 axis on tumor growth show conflicting results, and differences between different drugs were described. In a prostate cancer mouse model, CXCR4-positive PC3 tumors transfected with Bcl-2 or with empty vector were treated with the peptide antagonist CTCE-9908. Although Bcl-2–overexpressing tumors were sensitive to CXCR4 inhibition, the wild-type tumors showed no significant tumor growth delay on CTCE-9908 treatment [31]. In addition, AMD3100 monotherapy in other tumor types, such as a breast cancer metastatic mouse model [32] and a mouse model of acute myeloid leukemia [10], showed no differences in tumor growth between vehicle and AMD3100 treatment, although in the latter study, AMD3100 sensitized mice to bortezomib and cytarabine therapy. Two other studies using breast cancer mouse models [13,33] showed that treatment of the mice CTCE-9908 resulted in inhibition of the growth rate of primary tumor. In orthotopic glioma mouse models treatment with 1.25 mg/kg AMD3100 showed tumor growth inhibition in mice [34], whereas in other studies, treatment with doses of 10 and 5 mg/kg, respectively, did not [35,36]. On the basis of these studies, it seems that treatment with CTCE-9908 monotherapy might have more repressing effect on tumor growth than that with AMD3100. Our *in vivo* data are also supported by *in vitro* results, clearly showing that AMD3100 therapy alone does not have a cytotoxic effect on PC3-luc cells because they can be chemosensitized by CXCR4 inhibition only in the presence of stroma. Moreover, CXCL12 was not expressed by investigated cancer cells, excluding the possibility of the direct toxicity of AMD3100 due to the autocrine stimulation loop.

The rationale for the chemosensitization of prostate cancer by CXCR4 inhibition was provided by a study of acute promyelocytic leukemia mouse model. There, AMD3100 treatment resulted in mobilization of acute promyelocytic leukemia cells from the protective bone marrow microenvironment and increased tumor cell death from chemotherapy [6]. These preclinical studies provided proof-of-concept for phase 1/2 clinical trials in which patients with relapsed AML [37,38] and CLL [39] received intensive chemotherapy plus escalating doses of AMD3100. These studies demonstrated that AMD3100 combined with conventional chemotherapy is safe and does not affect hematological recovery, dispelling the common fear that mobilized normal HSCs will be affected by chemotherapy. Moreover, the 56% of the 1-year overall survival in 34 patients with AML treated with AMD3100 4 hours before mitoxantrone, etoposide, and cytarabine is a very promising result.

For solid tumors, the chemosensitization effect was also found in a transgenic breast cancer mouse model [13]. Mice treated with the combination docetaxel and CXCL12 analog CTCE-9908 showed a 38% decreased tumor volume—a larger effect than that observed with docetaxel alone. In glioma-bearing mice, treatment of AMD3100 synergized with subtherapeutic doses of 1,3-bis(2-chloroethyl)-1-nitrosourea, resulting in enhanced tumor regression [35]. In our study, AMD3100 sensitized both CXCR4 positive prostate cancer (PC3-luc) and breast cancer (MDA-MB-231) cells line after treatment with docetaxel, suggesting that targeting CXCR4 can be of additional value in a wide range of CXCR4-expressing cancers.

To analyze the potential relevance of our findings, we evaluated the CXCR4 expression levels in an unpaired set of prostate cancer patient specimens coming from either primary tumors or metastatic lesions. Our results showed that CXCR4 expression is higher in bone metastases compared with primary tumor tissue, whereas this up-regulation was not observed in such an extent in lymph node metastatic lesions. These results are compatible with the findings of Shiozawa et al. [14] and underscore the importance of the unique local microenvironment in the bone marrow for the biologic behavior of prostate cancer cells.

Interestingly, immunostaining of prostate tumors from the docetaxel-treated xenografted mice showed an up-regulation of CXCR4 receptors compared with the untreated tumors. Increased CXCR4 expression can potentially lead to cancer cells with heightened invasive capacity. Comparable results were found by targeting the VEGF pathway, either by anti-VEGFR2 antibody DC101, or multitargeted anti-angiogenic kinase inhibitor sunitinib, or by *Vegf-A* gene knockout in mouse models of pancreatic neuroendocrine carcinoma and glioblastoma [40]. Besides antitumor effects, tumor adaptation was concomitantly elicited and progression to higher stages of malignancy occurred, in some cases involving increased lymphatic and distant metastasis. These observations support further exploration of adding CXCR4 inhibitors to conventional therapy.

In summary, our study showed that CXCR4 inhibition sensitizes prostate cancer cells to docetaxel, both *in vitro* and *in vivo*. Current treatment strategies for metastasized prostate cancer with chemotherapy, radiotherapy, or hormonal therapy neglect the interaction of cancer cells with the protective microenvironment. Disrupting this interaction to sensitize cells to chemotherapy is therefore a potentially attractive strategy. Our findings should set the stage for clinical trials with combined treatment of conventional chemotherapy and CXCR4 antagonists, with the ultimate aim of improving treatment results in prostate cancer patients.

References

[1] Zlotnik A (2006). Chemokines and cancer. *Int J Cancer* **119**, 2026–2029.
[2] Akashi T, Koizumi K, Tsuneyama K, Saiki I, Takano Y, and Fuse H (2008). Chemokine receptor CXCR4 expression and prognosis in patients with metastatic prostate cancer. *Cancer Sci* **99**, 539–542.
[3] Scala S, Ottaiano A, Ascierto PA, Cavalli M, Simeone E, Giuliano P, Napolitano M, Franco R, Botti G, and Castello G (2005). Expression of CXCR4 predicts poor prognosis in patients with malignant melanoma. *Clin Cancer Res* **11**, 1835–1841.
[4] Yopp AC, Shia J, Butte JM, Allen PJ, Fong Y, Jarnagin WR, Dematteo RP, and D'Angelica MI (in press). CXCR4 expression predicts patient outcome and recurrence patterns after hepatic resection for colorectal liver metastases. *Ann Surg Oncol*.

[5] Salvucci O, Bouchard A, Baccarelli A, Deschenes J, Sauter G, Simon R, Bianchi R, and Basik M (2006). The role of CXCR4 receptor expression in breast cancer: a large tissue microarray study. *Breast Cancer Res Treat* **97**, 275–283.

[6] Burger JA and Peled A (2009). CXCR4 antagonists: targeting the microenvironment in leukemia and other cancers. *Leukemia* **23**, 43–52.

[7] Kucia M, Reca R, Miekus K, Wanzeck J, Wojakowski W, Janowska-Wieczorek A, Ratajczak J, and Ratajczak MZ (2005). Trafficking of normal stem cells and metastasis of cancer stem cells involve similar mechanisms: pivotal role of the SDF-1–CXCR4 axis. *Stem Cells* **23**, 879–894.

[8] Ishikawa F, Yoshida S, Saito Y, Hijikata A, Kitamura H, Tanaka S, Nakamura R, Tanaka T, Tomiyama H, Saito N, et al. (2007). Chemotherapy-resistant human AML stem cells home to and engraft within the bone-marrow endosteal region. *Nat Biotechnol* **25**, 1315–1321.

[9] Dillmann F, Veldwijk MR, Laufs S, Sperandio M, Calandra G, Wenz F, Zeller J, and Fruehauf S (2009). Plerixafor inhibits chemotaxis toward SDF-1 and CXCR4-mediated stroma contact in a dose-dependent manner resulting in increased susceptibility of BCR-ABL+ cell to imatinib and nilotinib. *Leuk Lymphoma* **50**, 1676–1686.

[10] Nervi B, Ramirez P, Rettig MP, Uy GL, Holt MS, Ritchey JK, Prior JL, Piwnica-Worms D, Bridger G, Ley TJ, et al. (2009). Chemosensitization of acute myeloid leukemia (AML) following mobilization by the CXCR4 antagonist AMD3100. *Blood* **113**, 6206–6214.

[11] Burger M, Hartmann T, Krome M, Rawluk J, Tamamura H, Fujii N, Kipps TJ, and Burger JA (2005). Small peptide inhibitors of the CXCR4 chemokine receptor (CD184) antagonize the activation, migration, and antiapoptotic responses of CXCL12 in chronic lymphocytic leukemia B cells. *Blood* **106**, 1824–1830.

[12] Kim M, Koh YJ, Kim KE, Koh BI, Nam DH, Alitalo K, Kim I, and Koh GY (2010). CXCR4 signaling regulates metastasis of chemoresistant melanoma cells by a lymphatic metastatic niche. *Cancer Res* **70**, 10411–10421.

[13] Hassan S, Buchanan M, Jahan K, Aguilar-Mahecha A, Gaboury L, Muller WJ, Alsawafi Y, Mourskaia AA, Siegel PM, Salvucci O, et al. (2011). CXCR4 peptide antagonist inhibits primary breast tumor growth, metastasis and enhances the efficacy of anti-VEGF treatment or docetaxel in a transgenic mouse model. *Int J Cancer* **129**, 225–232.

[14] Shiozawa Y, Pedersen EA, Havens AM, Jung Y, Mishra A, Joseph J, Kim JK, Patel LR, Ying C, Ziegler AM, et al. (2011). Human prostate cancer metastases target the hematopoietic stem cell niche to establish footholds in mouse bone marrow. *J Clin Invest* **121**, 1298–1312.

[15] Orimo A, Gupta PB, Sgroi DC, Arenzana-Seisdedos F, Delaunay T, Naeem R, Carey VJ, Richardson AL, and Weinberg RA (2005). Stromal fibroblasts present in invasive human breast carcinomas promote tumor growth and angiogenesis through elevated SDF-1/CXCL12 secretion. *Cell* **121**, 335–348.

[16] Olumi AF, Grossfeld GD, Hayward SW, Carroll PR, Tlsty TD, and Cunha GR (1999). Carcinoma-associated fibroblasts direct tumor progression of initiated human prostatic epithelium. *Cancer Res* **59**, 5002–5011.

[17] Ferlay J, Parkin DM, and Steliarova-Foucher E (2010). Estimates of cancer incidence and mortality in Europe in 2008. *Eur J Cancer* **46**, 765–781.

[18] Heidenreich A, Bellmunt J, Bolla M, Joniau S, Mason M, Matveev V, Mottet N, Schmid HP, van der Kwast T, Wiegel T, et al. (2011). EAU guidelines on prostate cancer. Part 1: screening, diagnosis, and treatment of clinically localised disease. *Eur Urol* **59**, 61–71.

[19] Mottet N, Bellmunt J, Bolla M, Joniau S, Mason M, Matveev V, Schmid HP, Van der Kwast T, Wiegel T, Zattoni F, et al. (2011). EAU guidelines on prostate cancer. Part II: treatment of advanced, relapsing, and castration-resistant prostate cancer. *Eur Urol* **59**, 572–583.

[20] Tannock IF, de Wit R, Berry WR, Horti J, Pluzanska A, Chi KN, Oudard S, Theodore C, James ND, Turesson I, et al. (2004). Docetaxel plus prednisone or mitoxantrone plus prednisone for advanced prostate cancer. *N Engl J Med* **351**, 1502–1512.

[21] de Bono JS, Oudard S, Ozguroglu M, Hansen S, Machiels JP, Kocak I, Gravis G, Bodrogi I, Mackenzie MJ, Shen L, et al. (2010). Prednisone plus cabazitaxel or mitoxantrone for metastatic castration-resistant prostate cancer progressing after docetaxel treatment: a randomised open-label trial. *Lancet* **376**, 1147–1154.

[22] Taichman RS, Cooper C, Keller ET, Pienta KJ, Taichman NS, and McCauley LK (2002). Use of the stromal cell–derived factor-1/CXCR4 pathway in prostate cancer metastasis to bone. *Cancer Res* **62**, 1832–1837.

[23] Meads MB, Hazlehurst LA, and Dalton WS (2008). The bone marrow microenvironment as a tumor sanctuary and contributor to drug resistance. *Clin Cancer Res* **14**, 2519–2526.

[24] de Vries EGE, Meijer C, Timmer-Bosscha H, Berendsen HH, de Leij L, Scheper RJ, and Mulder NH (1989). Resistance mechanisms in three human small cell lung cancer cell lines established from one patient during clinical follow-up. *Cancer Res* **49**, 4175–4178.

[25] Hwang RF, Moore T, Arumugam T, Ramachandran V, Amos KD, Rivera A, Ji B, Evans DB, and Logsdon CD (2008). Cancer-associated stromal fibroblasts promote pancreatic tumor progression. *Cancer Res* **68**, 918–926.

[26] Franco OE, Jiang M, Strand DW, Peacock J, Fernandez S, Jackson RS II, Revelo MP, Bhowmick NA, and Hayward SW (2011). Altered TGF-beta signaling in a subpopulation of human stromal cells promotes prostatic carcinogenesis. *Cancer Res* **71**, 1272–1281.

[27] Gilbert LA and Hemann MT (2010). DNA damage–mediated induction of a chemoresistant niche. *Cell* **143**, 355–366.

[28] Konopleva MY and Jordan CT (2011). Leukemia stem cells and microenvironment: biology and therapeutic targeting. *J Clin Oncol* **29**, 591–599.

[29] Taichman RS, Cooper C, Keller ET, Pienta KJ, Taichman NS, and McCauley LK (2002). Use of the stromal cell–derived factor-1/CXCR4 pathway in prostate cancer metastasis to bone. *Cancer Res* **62**, 1832–1837.

[30] De Clercq E (2009). The AMD3100 story: the path to the discovery of a stem cell mobilizer (Mozobil). *Biochem Pharmacol* **77**, 1655–1664.

[31] Porvasnik S, Sakamoto N, Kusmartsev S, Eruslanov E, Kim WJ, Cao W, Urbanek C, Wong D, Goodison S, and Rosser CJ (2009). Effects of CXCR4 antagonist CTCE-9908 on prostate tumor growth. *Prostate* **69**, 1460–1469.

[32] Smith MC, Luker KE, Garbow JR, Prior JL, Jackson E, Piwnica-Worms D, and Luker GD (2004). CXCR4 regulates growth of both primary and metastatic breast cancer. *Cancer Res* **64**, 8604–8612.

[33] Huang EH, Singh B, Cristofanilli M, Gelovani J, Wei C, Vincent L, Cook KR, and Lucci A (2009). A CXCR4 antagonist CTCE-9908 inhibits primary tumor growth and metastasis of breast cancer. *J Surg Res* **155**, 231–236.

[34] Rubin JB, Kung AL, Klein RS, Chan JA, Sun Y, Schmidt K, Kieran MW, Luster AD, and Segal RA (2003). A small-molecule antagonist of CXCR4 inhibits intracranial growth of primary brain tumors. *Proc Natl Acad Sci USA* **100**, 13513–13518.

[35] Redjal N, Chan JA, Segal RA, and Kung AL (2006). CXCR4 inhibition synergizes with cytotoxic chemotherapy in gliomas. *Clin Cancer Res* **12**, 6765–6771.

[36] Kioi M, Vogel H, Schultz G, Hoffman RM, Harsh GR, and Brown JM (2010). Inhibition of vasculogenesis, but not angiogenesis, prevents the recurrence of glioblastoma after irradiation in mice. *J Clin Invest* **120**, 694–705.

[37] Uy GL, Rettig MP, McFarland KM, Hladnik LM, Kulkarni S, Abboud CN, Cashen AF, Stockerl-Goldstein K, Vij R, Westervelt P, et al. (2008). Mobilization and chemosensitization of AML with the CXCR4 antagonist plerixafor (AMD3100): a phase I/II study of AMD3100 + MEC in patients with relapsed or refractory disease. *Blood* **112**, 678.

[38] Uy GL, Rettig MP, McFarland K, Hladnik L, Kulkarni S, Abboud CN, Cashen AF, Stockerl-Goldstein K, Vij R, Westervelt P, et al. (2009). A phase I/II study of chemosensitization with the CXCR4 antagonist plerixafor in relapsed or refractory AML. *Blood* **114**, 787.

[39] Andritsos L, Byrd JC, Jones JA, Hewes B, Kipps TJ, Hsu FJ, and Burger JA (2010). Preliminary results from a phase I dose escalation study to determine the maximum tolerated dose of plerixafor in combination with rituximab in patients with relapsed chronic lymphocytic leukemia. *Haematologica* **116**, 321.

[40] Paez-Ribes M, Allen E, Hudock J, Takeda T, Okuyama H, Vinals F, Inoue M, Bergers G, Hanahan D, and Casanovas O (2009). Antiangiogenic therapy elicits malignant progression of tumors to increased local invasion and distant metastasis. *Cancer Cell* **15**, 220–231.